18TH WORLD CONFERENCE ON EARTHQUAKE ENGINEERING
WCEE2024
MILAN

MILAN, ITALY
30TH JUNE - 5TH JULY 2024
www.wcee2024.it

# SEISMIC LOSS AND DOWNTIME ASSESSMENT OF COUPLED CLT SHEAR-WALL AND GLULAM MOMENT-RESISTING FRAME SYSTEM

Biniam Tekle Teweldebrhan[1,2] & Solomon Tesfamariam[3]

[1] PhD student, School of Engineering, The University of British Columbia, Okanagan Campus, 3333 University Way, V1V 1V7, Kelowna, BC, Canada, binitek@mail.ubc.ca

[2] Visiting PhD student, Department of Civil and Environmental Engineering, University of Waterloo, 200 University Ave W, N2L 3G1, Waterloo, ON, Canada

[3] Professor, Department of Civil and Environmental Engineering, University of Waterloo, 200 University Ave W, N2L 3G1, Waterloo, ON, Canada, solomon.tesfamariam@uwaterloo.ca

**Abstract**: *Amidst increasing recognition of the sustainable attributes and reduced carbon footprint of timber-based structural systems, dedicated efforts have been directed towards advancing this modern building practice. The CLT shear-wall and glulam moment-resisting frame (CLTW-GMRF) system is a notable addition in the design and evaluation of timber-based construction. Incorporating CLT balloon shear-walls, moment-resisting glulam frames, ductile beam-column joints, and buckling restrained brace hold-downs, this system demonstrates compliance with current building codes. However, recent seismic events have emphasized the need for earthquake-resilient structures that prioritize safety, minimize post-earthquake interventions, and promote usability. There-hence, the research proposed here explores the system resilience of a typical 10-story CLTW-GMRF system. A two-dimensional numerical model of the system is developed in OpenSees, and nonlinear response history analyses (NLTHA) are conducted using ground motions of various intensity levels selected based on the seismicity of Vancouver, British Columbia, Canada. Through the examination of the NLTHA, engineering demand parameters that capture global and local demand, and consequent system damage are determined. Moreover, incremental dynamic analysis is conducted to determine the probability of collapse of the system. Using FEMA P-58 methodology, the probabilistic seismic loss assessment, in terms of repair cost and time, is quantified. Accordingly, the post-earthquake recovery trajectory of the system is established, the resilience index of the system is predicted, and the key outcomes of the study with respect to the performance of its components are presented. Overall, this study contributes to a deeper understanding of the probabilistic seismic performance of the CLTW-GMRF system, providing engineers and researchers with valuable insights into its resiliency and proposing strategies for increased system performance.*

## 1. Introduction

The escalating trend of urbanization and its associated challenges have necessitated an increase in the construction of tall buildings. These structures serve as an efficient solution to counter urban sprawl and improve transportation efficiency. Nonetheless, the environmental impact of conventional construction materials, particularly in terms of $CO_2$ emissions and energy consumption, highlights the call for a shift in paradigm towards more sustainable, renewable, and eco-friendly construction materials (Milaj et al., 2017). In this context, timber, renowned for its inherent sustainability, has emerged as a promising alternative, attracting increasingly interest from researchers (Karacabeyli and Gagnon, 2019). This interest has catalysed the development of high-performance engineered wood products that improve various aspects of timber construction, including static and dynamic properties, fire resistance, and acoustic performance (Casagrande et al., 2022). Consequently, numerous timber-based structural systems are proposed, leading to a rapid change in building codes and design standards (Tesfamariam et al. 2021). A significant contribution in this

direction is the recently proposed Cross-Laminated Timber Shear-Wall and Glulam Moment Resisting Frame (CLTW-GMRF) system. The coupled system comprises CLT balloon shear-walls, CLT floor panels, glulam beams and columns, beam-column joints (BCJs) with replaceable steel dampers, buckling-restrained brace (BRB) hold-downs, and column-based joints (CBJs) with steel plates and lagscrewbolts. Developed for British Columbia (BC) Forestry Innovation Investment Ltd., the building details and general seismic design guidelines are provided in Tesfamariam and Teweldebrhan (2023) and Teweldebrhan and Tesfamariam (2023). In the later work, the authors investigate the system's performance with alternative BCJ and hold-down types: hybrid BCJs made up of post-tensioned tendons and mild steel dissipators, and self-centering energy dissipative hold-downs made up of pretensioned tendons and friction surfaces.

In the realm of earthquake engineering, different seismic design philosophies have been introduced and used to design structures, each representing a distinct strategy with specific design objectives. Despite the advancement in the seismic design of structures and deeper understanding of their behaviour under seismic events, our building codes still predominantly depend on prescriptive design approaches (Tesfamariam, 2022). While code-based design methods primarily focus on preventing collapse and safeguarding loss of life, they often lack provisions for resilient systems, leading to significant economic losses and extended downtime of buildings from post-seismic damage (Bruneau et al., 2003). In this scenario, the notion of seismic resilience takes on critical importance. Seismic resilience in buildings involves a comprehensive metric that extends beyond the immediate aftermath of earthquakes, embracing the entirety of the post-earthquake functional recovery process (Cimellaro et al., 2010). This concept, central to the performance-based earthquake engineering framework, underscores the critical role of loss and resilience assessment — an aspect that renders results more comprehensible and thus more actionable for clients and stakeholders (Mitrani-Reiser, 2007). There have been significant advancements in assessing and designing for seismic resilience in structures and infrastructure. Fundamental to these efforts are resources like FEMA P-58 (FEMA, 2018) and REDi™ (Almufti and Willford, 2013), which have shown significant success in accurately forecasting crucial decision variables, including economic losses, operational downtime, and casualties.

Despite the growing interest in timber construction, limited research delves into the seismic loss and resilience evaluation of these systems. For instance, Pei et al. (2017) developed a seismic design approach for resilient tall wood buildings. Wilson et al. (2021) explored the seismic loss of 5- and 12-story post-tensioned CLT buildings, while Furley et al. (2021) studied the recovery time of a 2-story timber structure. Medel-Vera and Contreras (2021) proposed a model based on seismic resilience and used it to access a 6-story CLT building. Most recently, You et al. (2023) conducted seismic loss and resilience assessment of a 20-story CLT coupled wall system. To expand upon the current knowledge, this study delves into the seismic loss and resilience assessment of the CLTW-GMRF system. A typical 10-story CLTW-GMRF structure is designed, considering a targeted wall-to-frame moment proportion ($MP$ = 60%-40%) and a seismic modification factor ($R_oR_d$) of 3. Utilizing OpenSees, a two-dimensional (2D) numerical model of the system is developed. Subsequently, nonlinear time history analyses (NLTHA) are conducted using a compilation of eight sets of 50 ground motion (GM) records, selected at different return periods to reflect the seismicity of Vancouver, BC - Canada. In addition, an incremental dynamic analysis (IDA) is performed to determine the collapse probability and develop the collapse fragility curve. The post-seismic state of the system is evaluated using the FEMA P-58 methodology, which provides estimates for the average repair cost, repair time, and the building's post-earthquake recovery trajectory. This study will not only broaden the understanding of the seismic behaviour of timber constructions but also emphasizes the critical importance of comprehensive loss and resilience evaluation in promoting the broader adoption of these eco-friendly systems in seismically active regions.

## 2. Methodology

This study follows the FEMA P-58 methodology (FEMA, 2018) to assess the seismic loss of CLTW-GMRF coupled system. Generally, this method follows a systematic procedure that evaluates seismic risks and consequences in terms of expected losses. The methodology can be summarized in 9 steps. Initially, structural model is established to accurately capture the building design. Once the model is in place, suites of GM, pertinent to the structure's geographical location and earthquake susceptibility, are selected. With this foundation set, NLTHA are undertaken to yield distributions of engineering demand parameters (EDPs) at the pre-defined seismic intensity levels. This analytical stage then transitions into the development of "R" number of realizations, using techniques such as Monte-Carlo Simulations to cover various possible scenarios. The next step then involves obtaining data on component fragility, alongside estimates of repair costs and

durations. Intensity-based loss estimation follows, leading to the derivation of a vulnerability function for the structure. This is then complemented by time-based loss projections, which detail the mean annual frequency of expected losses, both in terms of the likelihood of exceeding certain thresholds and the cumulative loss over a set of time frame. To provide a comprehensive measure of the structure's ability to recover from seismic events, the post-earthquake function recovery trajectory is developed, and its resilience index is quantified. Finally, the result from the preceding steps is summarized and the findings are interpreted in the context of the building's intended use, stakeholders' needs, and acceptable risk levels for decision making. The process is visually presented in Figure 1, and the detail procedures is elaborated in the FEMA-P58 documentation (FEMA, 2018). Note that time-based assessment is not part of this study.

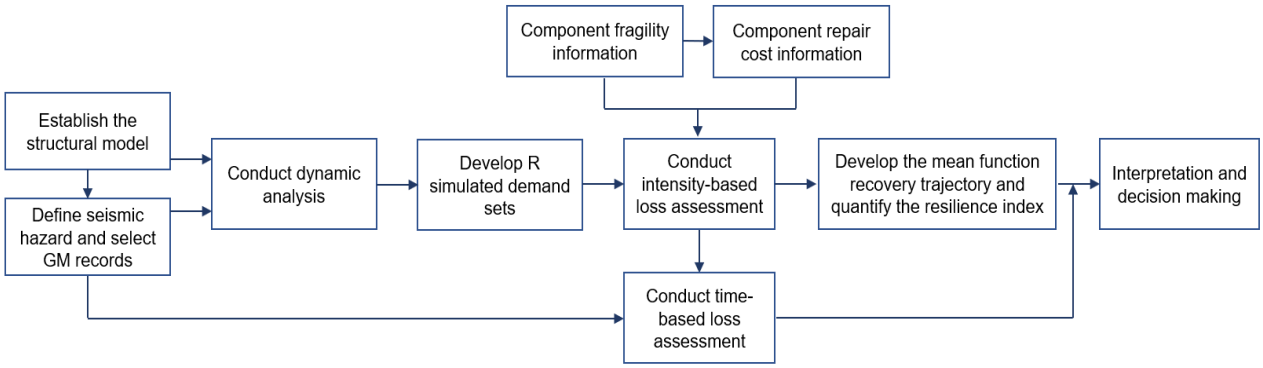


*Figure 1. Procedure for seismic loss and resilience assessment of a structural system.*

### 2.1 Building model and design information

As described in Section 1, this study extends the authors' previous work using the same building details, designs, models, and GM records. For an in-depth understanding of the system, the readers are referred to Tesfamariam and Teweldebrhan (2023) and Teweldebrhan and Tesfamariam (2023). However, this section briefly summarizes the structure's outline, seismic design methodology, and connection specifics.

*Building model*

The CLTW-GMRF system comprises CLT shear-walls, CLT floor panels, and glulam frame elements. The CLT floor panels are supported by the glulam frame elements and, when applicable, by the CLT shear-walls. Timber species Spruce-Pine-Fir and Douglas Fir-Larch are used for the CLT panel and glulam frame elements, respectively. The total height of the building is 30 m (each story is 3 m), and the length of each bay and CLT shear-wall is 4 m (Figure 2(a)). Structurally, the seismic resisting system of the building is the peripheral CLT balloon shear-wall and glulam frame elements (Figure 2(b)). These wall and frame systems are supplemented with energy-dissipative BRB hold-downs, and beam-column and column-base joints, respectively.

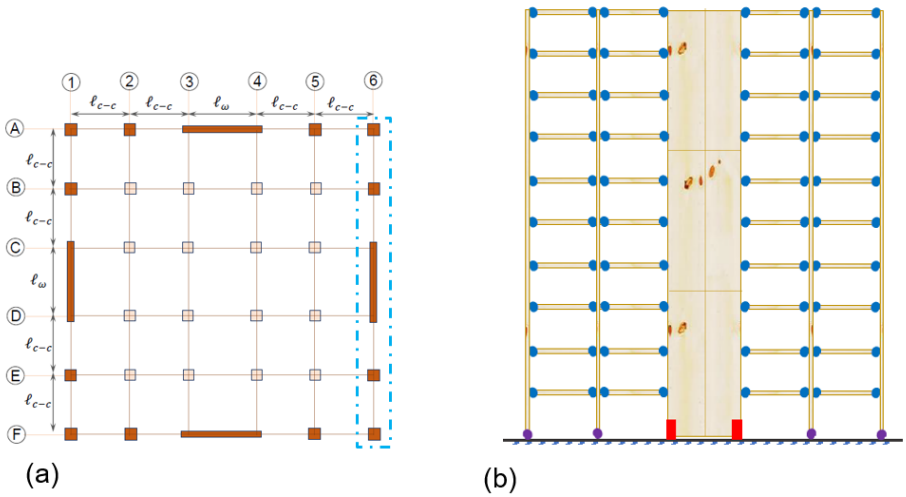


*Figure 2. CLTW-GMRF system: a) plan view and b) lateral load resisting system.*

*Seismic design*

Linear and nonlinear analysis models can be used to analyse wall-frame systems (Smith and Coull, 1991). In this study, targeted 60%-40% MP between the two systems (wall-to-frame) is chosen, and the seismic demand of the dual system is computed using equivalent static force procedure (NBC, 2020). Based on the targeted MP value, the continuous medium method is used to determine the seismic demand in each component of the system. ETABS program is then used to analyse the system. The force parameters of the timber elements are then extracted and designed following the CSA 086-19 (2019) standard. The designed dimensions of beams, columns, and CLT shear-wall (thickness) are 265 by 380 mm, 365 by 418 mm, and 267 mm, respectively. The complete seismic design procedure is provided in Tesfamariam and Teweldebrhan (2023).

*Connection details*

The BCJ, Wakashima et al. (2010), features a uniquely design (Figure 3(a)). A fuse-like, replaceable steel damper is connected to two end plates, which are firmly integrated into glulam frames through epoxy-bonded, threaded steel rods (Teweldebrhan and Tesfamariam, 2023). This design ensures that inelastic deformation occurs primarily within the damper, leaving the connection and frame elements largely unaffected and elastic. As a secondary energy dissipation component, the BRB hold-downs demonstrate high seismic performance with substantial ductility. These elements can be connected to the shear-walls at the base through epoxied threaded rods and a gusset plate, or bolts with side steel plates (Figure 3(b)). The moment demand in the CBJ was small and hence, any kind of conventional CBJ can be used. A CBJ tested by Mori et al. (2015) is used in this study. In this joint system, the column is inserted into a steel sleeve. Lagscrewbolts, embedded within the glulam columns, are bolted to a bottom steel plate, which in turn is welded to the steel sleeve (Figure 3(c)).

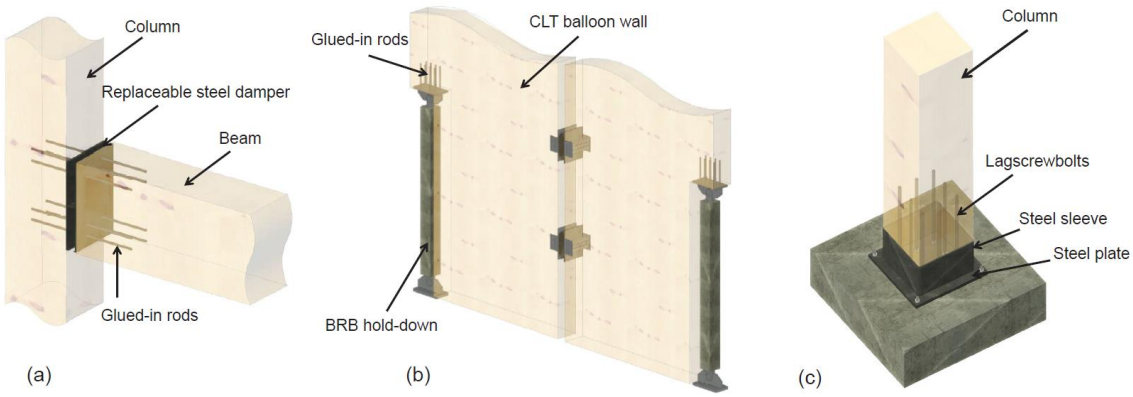


*Figure 3. Connection details: (a) beam-column joint; (b) BRB hold-downs; and (c) column-base joint.*

## 2.2 Numerical model

A 2D numerical model of the system is developed in OpenSees. The model is formed by assembling the CLT shear-walls, glulam frame elements, BCJs, CBJs, and hold-downs. The CLT wall panels are modelled as a single equivalent layer using OpenSees *ElasticIsotropic* material and *quad* elements (Teweldebrhan et al., 2023). The glulam frame elements are modelled using the *elasticBeamColumn* element feature (You et al., 2023). Experimental data from an existing study (Wakashima et al., 2010) is used for the BCJs and calibrated in OpenSees using *zeroLength Steel02* nonlinear rotation springs. The CBJs are modelled as *zeroLength* nonlinear rotation springs using the *Pinching4* model calibrated by Mori et al. (2015). The BRB hold-down is modelled using *zeroLength Steel01* material models. The contact between the wall and the base is modelled using *zeroLength uniaxial elastic no-tension (ENT)* material with large elastic stiffness value, assigned to the *ENT* spring under compression (Teweldebrhan et al., 2022). The P-Delta effects are captured using a leaning column, which is modelled using *elasticBeamColumn* elements. Based on the developed model, eigenvalue analysis is conducted, and the first three fundamental periods of the considered systems are computed. The detailed modelling parameter values can be found in Tesfamariam and Teweldebrhan (2023).

## 2.3 Seismic hazard and ground motion selection

Three seismic sources - crustal, in-slab, and interface - significantly contribute to seismic hazards in Vancouver. Probabilistic seismic hazard analysis (PSHA) is conducted, using an in-house tool developed by Tesfamariam et al. (2023). PSHA is performed with an in-house tool by Tesfamariam et al. (2023). The tool employs the NBC (2020) 6th generation seismic hazard model and uses a conditional mean spectra method

to give specific site hazard data and overall seismic hazard contributions. In this study, the first fundamental period of the prototype building is 1.87 s. As the FEMA P-58 standard (FEMA, 2018) recommends using GM records selected at eight different intensity levels, with at least seven GM records for each intensity, eight sets of 50 GM records (bi-directional) that possess the key features of the considered seismic sources are selected at $T_A$ = 2.0 s. The seismic hazard and records parameter (for 8 GM intensity levels) for the system at the assumed location is illustrated in Figure 4.

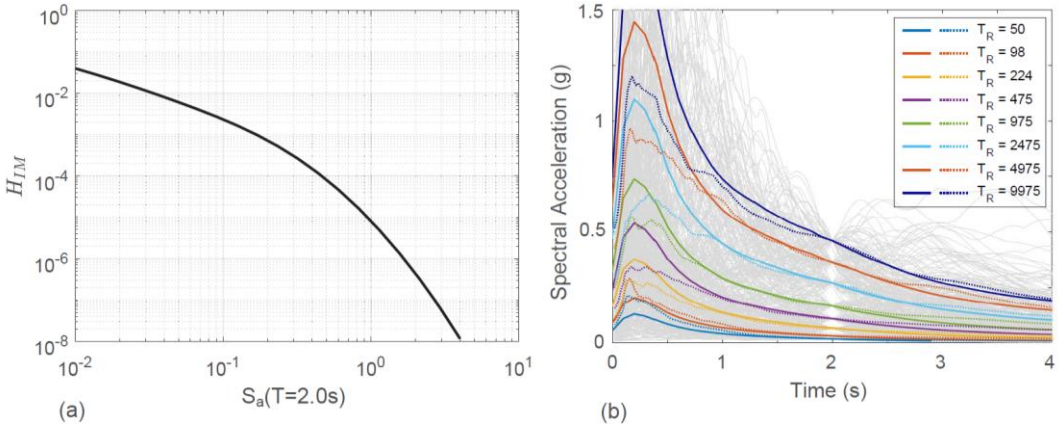


*Figure 4. GM-related plots: (a) seismic hazard curve; and (b) response spectra of selected GM records at different intensity levels (solid line: targeted response spectra and broken line: mean response spectra).*

## 3. Result and Discussion

### 3.1 System performance

Seismic performance of structures is often examined via NLTHA, allowing the extraction of component hysteretic responses and the EDPs of interest such as inter-story drift ratio (ISDR) and peak floor acceleration (PFA) responses. Figures 5(a–c) depict the average maximum ISDR (MaxISDR), residual ISDR (ResISDR), and PFA responses across the building. The results show averages from all GM records at varied intensity. Observations from Figure 5(a) indicate that the system's average MaxISDR values is well below 2.5%, except for GM records with a $T_R$ of 9975 which marginally reaches 2.5%. Notably, these drift ratio values are in line with the collapse prevention limit prescribed by the NBC (= 2.5%), even at higher GM intensity levels, demonstrating a satisfactory performance in achieving the building code objectives. Additionally, the mean values of ResISDR are below 0.5%, less than the maximum limit of 1% that would likely cause excessive downtime repairs of buildings. Furthermore, the average PFA values reveals that the maximum value occurs at the top floor (around 1.25g) from responses with return period of 9975 years.

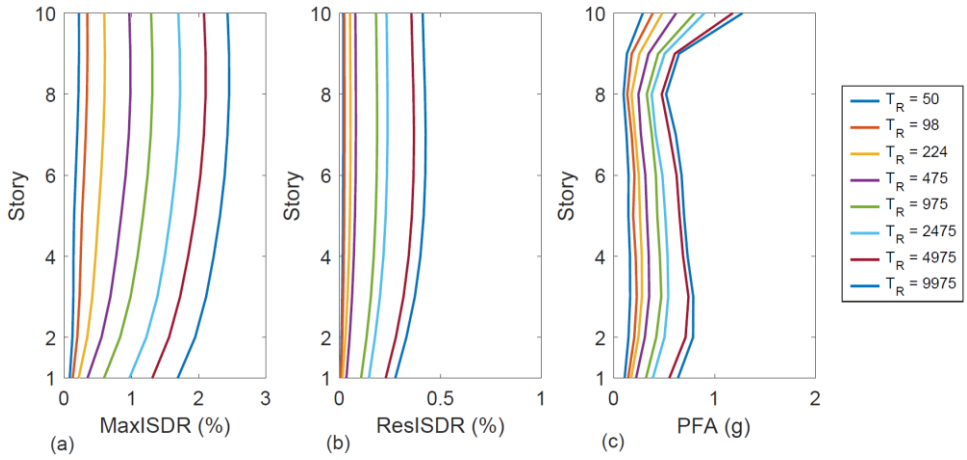


*Figure 5. Nonlinear time history results: (a) MaxISDR, (b) ResISDR, and (c) PFA.*

The FEMA P-58 methodology emphasizes the importance of assessing building performance up to collapse. A key component of this assessment is determining the collapse fragility curve, which probabilistically indicates the likelihood of collapse at different GM intensities. This curve not only informs the probabilistic consequences

such as casualties, repair costs, and downtime, but also aids in making informed decisions about repairs or reconstruction in line with cost considerations and safety standards. Determining the collapse probability often involves the use of IDA, where a series of scaled NLTHA are performed until collapse is reached. In this study, collapse of the system is assumed to occur around 4.8% (≈5%), as determined by Teweldebrhan and Tesfamariam (2023). Moreover, a 5% damped spectral acceleration at the first fundamental period of the system ($S_a(T_1)$) is chosen as an intensity measure (IM), for the GM records chosen at $T_R$ = 2475 years. With this, the analysis is performed, and the collapse spectral acceleration values are then used to develop collapse fragility curves, assuming a lognormal distribution. Typical IDA and fragility curves for the CLTW-GMRF system are shown in Figure 6. Note that, assuming the structure model has fair to medium quality rating, an epistemic uncertainty of 0.35 is considered while developing the collapse fragility.

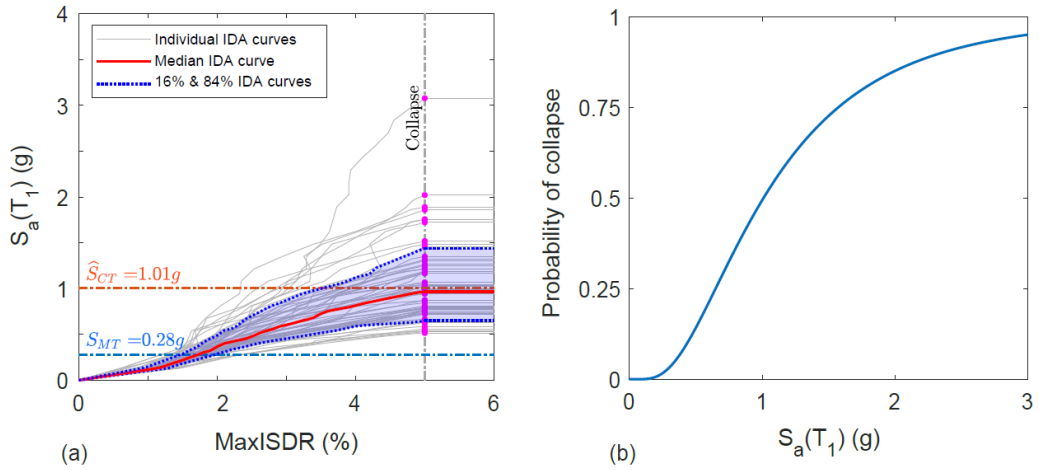


*Figure 6. (a) IDA result; and (b) collapse fragility curve.*

### 3.2 Component definitions

In assessing the seismic risks of the building system, it's imperative to define its components and establish their potential damage states (DSs). The FEMA P-58 framework (FEMA, 2018) characterizes the likelihood of surpassing a given DS and its subsequent implications using a component fragility function. This section provides a detailed overview of the components and highlights the fragility data crucial for the loss assessment.

*Structural components*

Although the FEMA P-58 documentation (FEMA, 2018) provides a library of ready-for-use fragility functions for common structural components, the fragility functions for the specified structural components of the CLTW-GMRF system such as replaceable steel damper BCJs, BRB hold-downs, balloon-type CLT shear-walls, and the conventional CBJs are not provided. In the absence of these functions, FEMA P-58 permits users to employ or develop fragility models from existing literature or experimental data. Consequently, this study develops fragility functions from existing research, and utilizes when applicable from literature and FEMA P-58, with justifiable assumptions to define the fragility function of the structural components.

The experimental test conducted by Wakashima et al. (2010) showcased distinct BCJ behaviour under cyclic loading conditions. Specifically, the joint was observed to yield at approximately 0.01 rad and maintained a stable hysteretic curve up to about 0.04 rad, further cycling (to a rotation limit of 0.05 rad) resulted in complete failure of the joint system. An independent study by Gohlich et al. (2018) confirmed a similar range of limits and joint behaviour for a BJC made of replaceable steel links with self-tapping screw connections. With the later, extensive experimental results are provided under various conditions. As per Gohlich et al. (2018), around 0.02 rad, the joint started to show out-of-plane local buckling of the web which becomes excessive when the rotation reaches 0.03 rad. Around 0.04 rad, local buckling of the flanges occurred along with gap openings between the columns and the column side plates. Accordingly, these stated three damage conditions are defined as three DSs in this study. For the consequence and repair solutions, FEMA P-58 is referenced for BCJs in steel structures (reduced beam section, RBS) that exhibited similar damage behaviours, with the exception that the DS begins at 0.03 rad. For both DS1 and DS2, the potential solution would likely involve repairing the joint by heat straightening of the buckled web. For DS3, repair would be more intensive, requiring the removal and replacement of distorted and/or fractured portion of the joint. In term of consequences, for

DS1 utilizes half of the estimated consequences designated for DS1 in RBS, For DS2, the entirely of the damage consequences from DS1 of RBS are considered. Likewise, the consequences of DS3 are drawn directly from FEMA P-58 consequence for DS2 in RBS.

Although fragility function for BRB braces are available in FEMA P-58, specific functions for BRB hold-downs remain elusive. Addressing this gap, You et al. (2023) developed a fragility function for BRB hold-downs derived from the BRB data in FEMA P-58. Notably, while BRBs are described by a single DS in FEMA P-58, You et al. adapted this by leveraging the relationship between ISDR and BRB axial strain. The authors adjusted the median ISDR value for standard diagonal BRBs (=2%) to account for vertically positioned BRB hold-downs. Given geometric considerations and the assumption of infinitesimal deformations, the authors deduced the axial strain threshold for the singular DS for BRB hold-downs to be half of the ISDR value (=1%). This study also adopts the three DSs for balloon-type CLT shear-walls identified by the authors, alongside their respective repair measures and consequence details.

Experimental test result for the CBJ system is provided in Mori et al. (2015). Generally, the base system exhibited pinching hysteretic response with failure occurred due to the complete pullout of lagscrews from the timber column. From the provided hysteretic response and damage condition in Mori et al. (2015), three DSs are defined in this study. At the onset of DS1 (around 0.0045 rad), the joint might exhibit partial tearing of the steel sleeve or potential crack initiation at the intersection of the steel sleeve and steel plate. The likelihood of this failure is small and assumed as 5%. To address this, weld repairs to any discernible cracks can be conducted, and in certain scenarios, a replacement of the steel plate might be necessitated. For DS2 (around 0.02 rad), the lagscrewbolts undergo a non-linear (post-yielding) deformation. The remedy involves the installation of new lagcrewbolts. DS3 (around 0.032 rad), the most severe of the states, is characterized by a near-complete pullout of the lagscrews from the timber column, signalling an imminent loss of vertical load resistance. This would require a comprehensive repair which includes the complete replacement of the steel plate and the installation of new lagcrewbolts. Like with the BCJs, consequences associated with CBJs are inferred from FEMA P-58's prescribed damage consequences designated for steel column base plates. Table 1 has summarized the DSs and the consequences of the damages for all the structural components.

*Table 1: Damage fragility and consequence details for structural components of CLTW-GMRF system*

| Component type | ID | EDP type | Damage state | Median (%) | Dispersion | Repair cost ($*) | Repair time (days) |
|---|---|---|---|---|---|---|---|
| Replaceable steel damper BCJs | B1035.071 | Joint rotation angle | DS1 | 2.0% | 0.30 | 7395-10875 | 4.35-6.40 |
| | | | DS2 | 3.0% | 0.30 | 14790-21750 | 8.70-12.79 |
| | | | DS3 | 4.0% | 0.30 | 24905-36625 | 14.65-21.54 |
| BRB hold-downs | B1033.201 | Axial strain | DS1 | 1.0% | 0.40 | 33226-53992 | 22.0-36.0 |
| CLT shear-wall | B1081.001 | Story drift ratio | DS1 | 0.3% | 0.44 | 1840-2990 | 1.8-2.9 |
| | | | DS2 | 0.5% | 0.30 | 2337-3330 | 2.3-3.2 |
| | | | DS3 | 2.7% | 0.16 | 3825-5400 | 3.7-5.2 |
| Conventional CBJs | B1031.201 | Joint rotation angle | DS1 | 0.45% | 0.40 | 509-827 | 0.5-0.8 |
| | | | DS2 | 2.0% | 0.40 | 10176-16536 | 9.88-16.05 |
| | | | DS3 | 3.2% | 0.40 | 15264-10812 | 10.49-14.82 |

*: Repair costs are given per 100 sq. ft for CLT shear-wall and per unit quantity for the rest of the structural components.

*Non-structural components*

The quantity of non-structural components and building contents for the considered system are estimated using the FEMA P-58 Normative Quantity Estimation Tool (FEMA, 2018), based on the building plan area and occupancy type. As outlined in Section 2.1, the building is designed for residential use, with all stories identified as an apartment occupancy type. While certain components are exclusive to specific story level, others span across the building stories. Components such as wall partitions and curtain walls are directional, reacting solely to vibrations in their specific seismic excitation direction. Conversely, nondirectional components have DSs determined by the maximum EDP observed in both directions. The total quantities for each non-structural component are summarized in Table 2.

*Table 2: Quantity of non-structural components*

| Pact fragility ID. | Name | Performance group quantity | PACT Unit | Dispersion | Floors |
|---|---|---|---|---|---|

| | | | | | |
|---|---|---|---|---|---|
| B2022.001 | Curtain walls | 21.53 | 30 SF | 0.6 | All |
| B3011.011 | Concrete tile roof | 13.78 | 100 SF | 0.9 | Roof |
| C1011.001a | Wall partition | 5.17 | 100 LF | 0.3 | All |
| C2011.001a | Stairs | 0.52 | 1 EA | 0.4 | All |
| C3011.001a | Wall finishes | 1.64 | 100 LF | 0 | All |
| D1014.011 | Traction elevator | 1.46 | 1 EA | 0.8 | 1st |
| D2021.011a | Potable water pining | 0.46 | 1000 LF | 0.4 | All |
| D3041.011a | HVAC ducting | 0.26 | 1000 LF | 0.6 | All |
| D3041.031a | HVAC drops/diffusers | 3.44 | 10 EA | 0.4 | All |
| D3041.041a | Variable air volume box | 1.72 | 10 EA | 0 | All |
| D4011.021a | Fire sprinkler water piping | 0.95 | 1000 LF | 0.1 | All |
| D4011.031a | Fire sprinkler drop | 0.52 | 100 EA | 0.1 | All |
| D5011.011a | Transformer | 11.7 | 1 EA | 0.5 | 1st |
| D5012.021a | Low voltage switchgear | 0.02 | 225 AP | 0.3 | All |
| D5012.031a | Distribution panel | 3.05 | 1 EA | 0.2 | 1st |

EA: each; SF: square feet; LF: linear foot; HVAC: heating, ventilation, and air conditioning; AP: ampere.

### 3.3 Intensity-based loss assessment

In this study, intensity-based loss assessments are carried out for GM records at varying intensity levels using the PELICUN Python library (Zsarnóczay and Zhong, 2020). For each GM intensity, 1000 Monte-Carlo simulations are executed to generate EDPs. The building is deemed collapsed if the simulated MaxISDR exceeds 5% and becomes irreparable if the average ResISDR exceeds 1%. If the building either collapses or becomes irreparable due to significant MaxISDR or ResISDR, its repair cost and time will be equal to the entire building reconstruction cost and duration, respectively. Otherwise, the structure becomes repairable, and its repair costs is determined from the sum of all vulnerable structural and non-structural components.

For the loss assessment, it is assumed that the reconstruction period of 548 days and the reconstruction cost of the building as US$9.30 million (calculated at a rate of US$ 216 per sq. ft as per Sorathiya (2019)). Moreover, parallel repair approach is employed, assuming there are a maximum of four workers per floor will be available for post-earthquake repairs. With these considerations, Figure 7 displays the cumulative distribution functions (CDFs) of repair costs and durations for each GM intensity level. Figure 7(a) indicates that the probability of repair costs exceeding reconstruction costs remains minimal, suggesting repair is more viable than total reconstruction. In all GM scenarios, the highest anticipated repair cost, for $T_R$ = 9975 years, approximates at US$4.58 million, contrasting with the US$9.30 million reconstruction cost. Similarly, estimated repair durations are shorter than the 548-days reconstruction period, varying from about 8 to 198 days based on the GM level. From a cost perspective, the probability of reconstruction is approximately 0% and 2% for design and maximum considered earthquake level, respectively. The same probabilities remain consistent when assessed from a time frame standpoint.

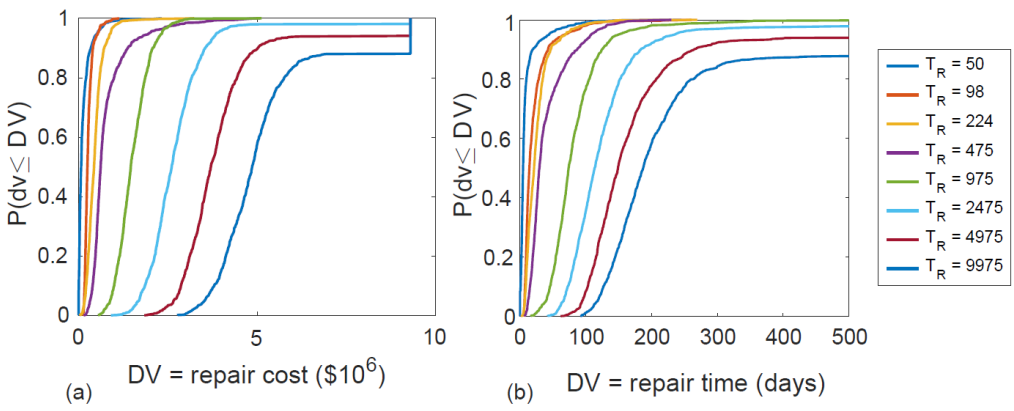


*Figure 7. Probability of non-exceedance: a) repair cost, and b) repair time.*

To identify components that significantly contribute to the loss assessment, component losses at various story and GM intensity levels can be readily obtained. Figure 8(a) illustrates the repair costs of structural and non-structural components across the building story levels. For each story, four bars represent the four GM intensity levels with $T_R$ of 98, 475, 2475, and 9975 years. The first story incurs the highest repair cost due to the presence of BRB hold-downs, CBJs, elevators, distribution panels, and transformers. As we move up the building, the repair cost rises (excluding the 1st story). This increase is primarily due to the escalating repair costs of the structural components, especially the BCJs. The response of the BCJs intensifies with higher stories, a trend also observed in the distribution of MaxISDR, as shown in Figure 4(a). Conversely, the top story has a relatively higher repair cost compared to the intermediate stories, primarily because of additional non-structural components on the roof, though it's still lower than the first story's repair cost.

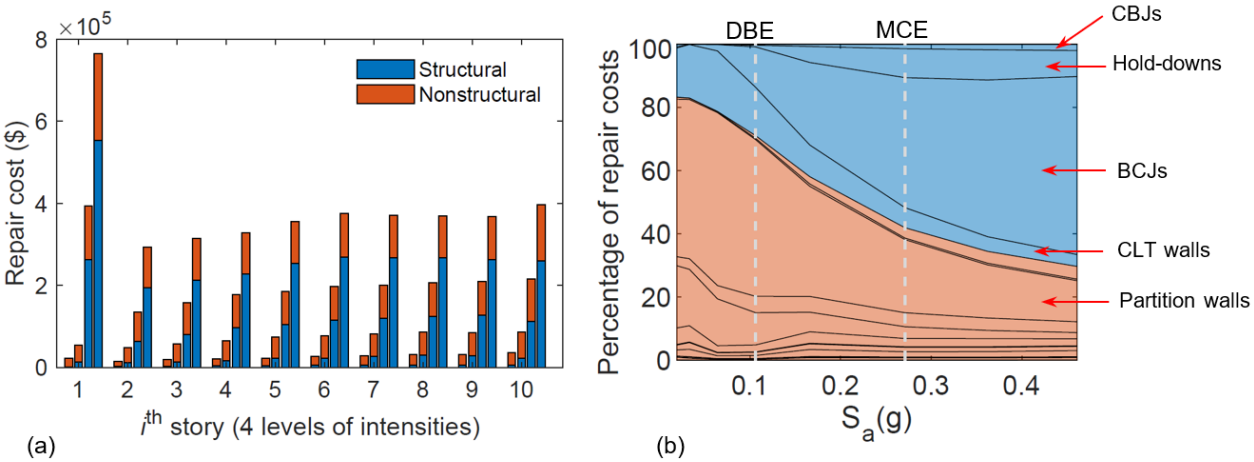


*Figure 8. Repair cost: a) story levels distribution and b) percentage contribution from different components*

The percentage ccontribution for the repair cost from the different structural and non-structural components, at different GM intensity levels, is summarized in Figure 8(b). At lower GM intensity levels, the percentage of contribution of non-structural components was dominant and the major contribution was from C1011.011a (partition walls). As the GM intensity level increase, the damage in structural components increases. Notably, the contribution of BCJs becomes the highest. When zoomed at the design and maximum considered earthquake levels, the percentage of contribution from structural components were 29% and 58% respectively. The corresponding percentage contribution from BCJs were 13% and 41%, corresponding to of the repair cost of structural components, respectively. Given the contribution level of BCJ and their replaceable nature during damage, the CLTW-GMRF system building has a good replaceable property.

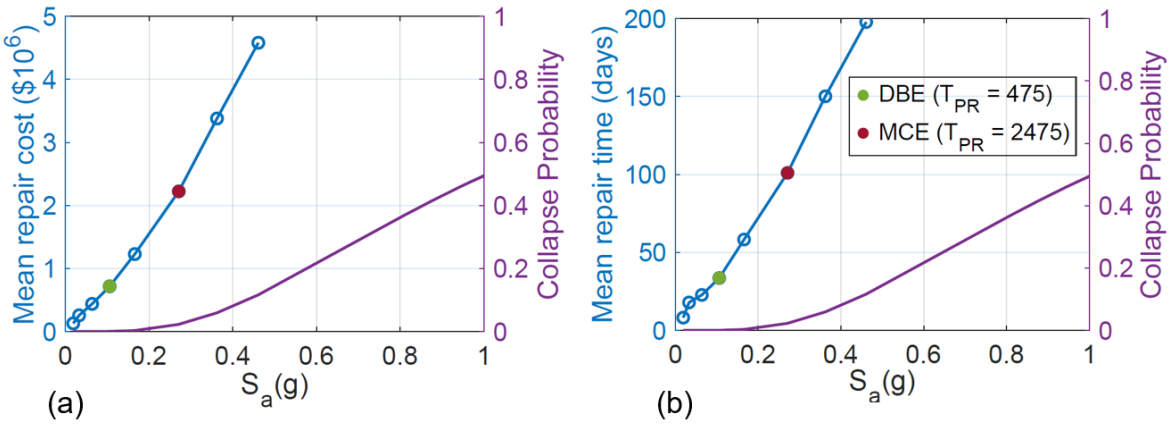


*Figure 9. a) Mean repair cost and b) mean repair time.*

Mean repair cost and repair time (with 50% probability of non-exceedance) with respect to spectral accelerations are presented in Figure 9. As can be seen from Figure 9(a), for GM intensities with $T_R$ period of 975 years and less, most seismic losses are caused by damaged components, while contribution from collapse is negligible, because collapse probability is almost 0%. At the design and maximum considered earthquake

levels, the mean repair cost is US$0.72 million and US$2.22 million, which are about 8% and 24% of the reconstruction cost, respectively. Similarly, from Figure 9(b), it can be noted that the mean repair time is about 34 and 101 days, respectively. Thus, in both these GM intensities, repair cost is smaller than the reconstruction cost, and repair time is shorter than the reconstruction time, which implies that building repair is the most likely scenario for the designed CLTW-GMRF system.

### 3.4 Seismic resilience assessment

The seismic resilience of a structure can be predicted by observing its post-earthquake recovery trajectory (Bruneau et al., 2003; Cimellaro et al., 2010). A building function at a certain time after earthquake, Q(t), is determined to prepare the recovery trajectory of a system. For the residential building studied here, Q(t) reflects the housing function: a value of 1 when it's habitable and 0 otherwise. Notably, a building can become habitable before all damages are fully repaired, making functional recovery often quicker than the complete repair. FEMA (2020) has provided a multiplier (a factor ≤1) for converting repair time into functional recovery time, dependent on damage extent. For complete damage (MaxISDR > 2.5%), the multiplier is 1, equating the functional recovery time to the repair time since the building is likely to be reconstructed. For minimal damage (MaxISDR < 1.5%), the multiplier is 0, suggesting the damage won't affect the habitability of the system. For moderate damage (MaxISDR between 1.5% and 2.5%), the multiplier is 0.5, meaning the functional recovery time is half of the repair time. Given the inherent uncertainties in earthquakes and their subsequent effects, the mean value of Q(t) is derived from Monte-Carlo simulations for different GM intensity levels, as illustrated in Figure 10.

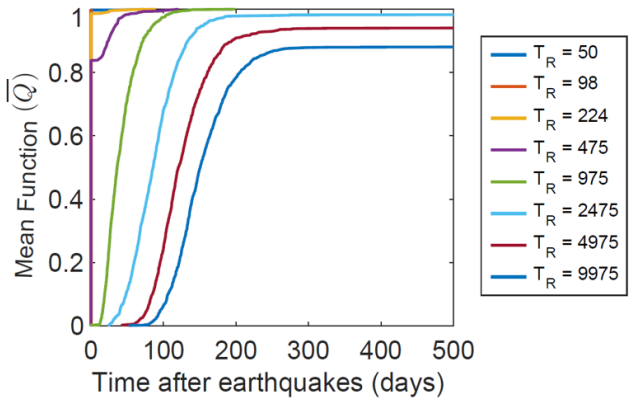


*Figure 10. Mean functional recovery of CLTW-GMRF system at different GM intensity levels.*

Quantitatively, the seismic resilience of the system is also examined by using a resilience index (R), defined as (Bruneau et al., 2003; Cimellaro et al., 2010):

$$\mathrm{R} = \frac{1}{T_c} \int_{t=0}^{T_c} \bar{Q}(t)\, dt$$

where $T_c$ is control time for calculating resilience index (= 500 days). Utilizing this formula, Table 3 lists the total repair time, average functional recovery duration, and resilience index relevant to various GM intensity levels. Notably, the system's average functional recovery times for the design and maximum considered earthquake levels are 5.21 and 95.80 days, respectively. Their corresponding resilience indices of 0.99 and 0.81 highlight the structure's commendable resilience against expected seismic events.

*Table 3. Seismic resilience indices under different intensities*

| **Return Period (years)** | **50** | **98** | **224** | **475** | **975** | **2475** | **4975** | **9975** |
|---|---|---|---|---|---|---|---|---|
| Mean repair time (days) | 8.14 | 17.88 | 22.72 | 33.57 | 58.29 | 101.04 | 150.17 | 197.86 |
| Mean function loss (days) | 0 | 0 | 0.46 | 5.21 | 41.83 | 95.80 | 149.97 | 197.86 |
| Resilience | 1.00 | 1.00 | 1.00 | 0.99 | 0.92 | 0.81 | 0.70 | 0.60 |

## 4. Summary and conclusion

In the modern construction industry, timber-based structural systems are becoming popular choice due to urban densification and demand for sustainable materials. The CLTW-GMRF is a newly introduced timber structural system. Earlier works by the authors covered its general behaviour and seismic design. This paper delves into the seismic loss and resilience of this dual system, focusing on a 10-story CLTW-GMRF designed with a 60% to 40% wall-to-frame moment proportion and a seismic modification factor of 3. The study uses the FEMA P-58 methodology and quantifies the system's intensity-based loss assessment and functional recovery. Key findings from this research include:

- The CLTW-GMRF system showcased significant resilience under seismic events. Repairing the structure post an earthquake is often more viable than a complete reconstruction.
- The BCJs, due to their replaceable nature, present a strategic advantage in the design, offering an efficient recovery route after seismic events.
- Non-structural components significantly influence repair costs at lower seismic intensities, but as the intensity increases, structural components become the primary contributors to the costs.
- The resilience assessment reinforces the effectiveness of the CLTW-GMRF design, underlining its capability to regain functionality quickly after an earthquake.

Overall, this study offers comprehensive insights into the seismic performance of the CLTW-GMRF system, emphasizing the value of component-level analysis and the importance of resilience assessments in building designs. The findings underline the potential benefits of the CLTW-GMRF system as a seismic-resistant structure, especially in earthquake-prone areas. This study is expected to provide engineers and researchers with valuable insights into the system and proposing strategies for increased system resilience performance.

## 5. References

Almufti I., and Willford M. (2013). REDi™ rating system: *Resilience-based earthquake design initiative for the next generation of buildings*. Report, Arup Co.

Bruneau M., Chang S.E., Eguchi R.T., Lee G.C., O'Rourke T.D., Reinhorn A.M., Shinozuka M., Tierney K., Wallace W.A., and von Winterfeldt D. (2003). A framework to quantitatively assess and enhance the seismic resilience of communities. *Earthquake Spectra* 19(4): 733–752.

Casagrande D., Brandon D., D'Arenzo G., and Viau C. (2022). *Design of taller timber buildings subjected to accidental loads: a state-of-the-art review*. European Cooperation in Science and Technology (COST Action CA20139).

Cimellaro G.P., Reinhorn A.M., and Bruneau M. (2010). Framework for analytical quantification of disaster resilience. *Engineering Structures* 32(11): 3639–3649.

CSA (2019). *Standard CSA 086-19: Engineering Design in Wood*. Canadian Standards Association, Mississauga, Canada.

FEMA (2018). *Seismic performance assessment of buildings*. Report, Applied Technology Council (ATC). Redwood City, CA.

Furley J., van de Lindt J.W., Pei S., Wichman S., Hasani H., Berman J.W., Ryan K., Daniel Dolan J., Zimmerman R.B., and McDonnell E. (2021). Time-to-functionality fragilities for performance assessment of buildings. *Journal of Structural Engineering* 147(12): 04021217.

Gohlich R., Erochko J., and Woods J. E. (2018). "Experimental testing and numerical modelling of a heavy timber moment-resisting frame with ductile steel links." *Earthquake Engineering & Structural Dynamics*, 47(6), 1460–1477.

Karacabeyli E., and Gagnon S. (2019). *Canadian CLT Handbook 2019 Edition*. Vancouver, BC, Canada: FPInnovations.

Medel-Vera C., and Contreras M.C. (2021). Resilience-based predictive models for the seismic behavior of mid-rise, base-isolated CLT buildings for social housing applications in Chile. *Journal of Building Engineering* 44: 103397.

Milaj K., Sinha A., Miller T.H., and Tokarczyk J.A. (2017). Environmental utility of wood substitution in commercial buildings using life-cycle analysis. *Wood and Fiber Science* 49(3): 338–358.

Mitrani-Reiser J. (2007). *An ounce of prevention: Probabilistic loss estimation for performance-based earthquake engineering*. PhD Thesis, California Institute of Technology, Pasadena, CA.

Mori T., Nakatani M., and Tesfamariam S. (2015). Performance of semirigid timber frame with Lagscrewbolt connections: experimental, analytical, and numerical model results. *International Journal of Advanced Structural Engineering (IJASE*), 7, 387–403.

NBC (2020). *National Building Code of Canada 2020.* National Research Council of Canada (NRCC), Ottawa, Canada.

Pei S., van de Lindt J., Barbosa A.R., Berman J., Blomgren H.E., Dolan J., McDonnell E., Zimmerman R., Fragiacomo M., and Rammer D. (2018). Full-scale shake table test of a two-story mass-timber building with resilient rocking walls. In: Proceedings, *16th European conference on earthquake engineering*. Thessaloniki, pp. 1–10.

Smith, S.B. and Coull, A. (1991). *Tall Building Structures: Analysis and Design.* John Wiley amp; Sons, Inc.

Sorathiya R. (2019). *Literature review of cost information on mid-rise mass-timber building projects*. Report, SALA UBC, Vancouver, BC, Canada.

Tesfamariam S. (2022). Performance-based design of tall timber buildings under earthquake and wind multi-hazard loads: Past, present, and future. *Frontiers in Built Environment* 8: 848698.

Tesfamariam S., and Teweldebrhan B.T. (2023). *Seismic Design of Tall Timber Building with Dual CLT-Shear Wall and Glulam Moment Resisting Frame Systems.* Faculty Research and Publications. https://dx.doi.org/10.14288/1.0431446

Tesfamariam S., Badal P.S., and Goda K. (2023). *Seismic Hazard and Ground Motion Selection for Response History Analysis per the National Building Code of Canada 2020*. UBC Faculty Research and Publications. https://dx.doi.org/10.14288/1.0431445.

Tesfamariam S., Skandalos K., and Teweldebrhan B.T. (2021). *Design of Tall-Coupled-Wall Timber Building: Energy Dissipating Coupling Beams.* Faculty Research and Publications. https://dx.doi.org/10.14288/1.0403817

Teweldebrhan B.T., and Tesfamariam S. (2023). Seismic Design of CLT Shear-Wall and Glulam Moment-Resisting Frame Coupled Structure. *Journal of Structural Engineering*, 149(12), 04023169.

Teweldebrhan B.T., Goda K., De Risi R., and Tesfamariam, S. (2023). Multi-variate Seismic Fragility Assessment of CLT Coupled Wall Systems. *Earthquake Spectra*, 87552930231190687.

Teweldebrhan B.T., Popovski M., McFadden J.B., and Tesfamariam S., (2022). Development of ductility-related modification factor for CLT-coupled wall buildings with replaceable shear link coupling beams. *Canadian Journal of Civil Engineering*, *50*(5), pp.362-374.

Wakashima Y., Okura K., and Kyotani K. (2010). Development of ductile semi-rigid joints with lag screw bolts and glued-in rods. *Proceedings of the 11th World Conference on Timber Engineering-WCTE 2010*.

Wilson A.W., Phillips A.R., Motter C.J., Lee J.Y., and Dolan J.D. (2021). Seismic loss analysis of buildings with post-tensioned cross-laminated timber walls. *Earthquake Spectra* 37(1): 324–345.

You T., Teweldebrhan B.T., Wang W., and Tesfamariam S. (2023). Seismic loss and resilience assessment of tall-coupled cross-laminated timber wall building. *Earthquake spectra*, 87552930231152512.

Zsarnoczay A., and Zhong K. (2020). PELICUN. Available at: https://nheri-simcenter.github.io/pelicun.